

2017-05-17

## Extending Chemical Perturbations Of The Ubiquitin Fitness Landscape In A Classroom Setting

David Mavor  
*University of California, San Francisco*

*Et al.*

Let us know how access to this document benefits you.

Follow this and additional works at: [https://escholarship.umassmed.edu/faculty\\_pubs](https://escholarship.umassmed.edu/faculty_pubs)



Part of the Amino Acids, Peptides, and Proteins Commons, Bioinformatics Commons, Ecology and Evolutionary Biology Commons, and the Genetic Phenomena Commons

---

### Repository Citation

Mavor D, Bolon DN, Kampmann M, Fraser JS. (2017). Extending Chemical Perturbations Of The Ubiquitin Fitness Landscape In A Classroom Setting. University of Massachusetts Medical School Faculty Publications. <https://doi.org/10.1101/139352>. Retrieved from [https://escholarship.umassmed.edu/faculty\\_pubs/1541](https://escholarship.umassmed.edu/faculty_pubs/1541)

Creative Commons License



This work is licensed under a [Creative Commons Attribution 4.0 License](https://creativecommons.org/licenses/by/4.0/).

This material is brought to you by eScholarship@UMMS. It has been accepted for inclusion in University of Massachusetts Medical School Faculty Publications by an authorized administrator of eScholarship@UMMS. For more information, please contact [Lisa.Palmer@umassmed.edu](mailto:Lisa.Palmer@umassmed.edu).

1 **Research Advance:**  
2 **Extending chemical perturbations of the Ubiquitin fitness landscape**  
3 **in a classroom setting**

4  
5 *Coordinators:* David Mavor, Kyle A. Barlow

6 *TAs:* Daniel Asarnow, Yuliya Birman, Derek Britain, Weilin Chen, Evan M. Green, Lillian R.  
7 Kenner, Bruk Mensa, Leanna S. Morinishi, Charlotte Nelson, Erin M. Poss, Pooja Suresh, Ruilin  
8 Tian

9 *Students:* Taylor Arhar, Beatrice Ary, David Bauer, Ian Bergman, Rachel Brunetti, Cynthia Chio,  
10 Shizhong Dai, Miles Dickinson, Susanna Elledge, Cole Helsell, Nathan Hendel, Emily Kang,  
11 Nadja Kern, Matvei Khoroshkin, Lisa Kirkemo, Greyson Lewis, Kevin Lou, Wesley Marin, Alison  
12 Maxwell, Peter McTigue, Douglas Myers-Turnbull, Tamas Nagy, Andrew Natale, Keely Oltion,  
13 Sergei Pourmal, Gabriel Reder, Nicholas Rettko, Peter Rohweder, Daniel Schwarz, Sophia Tan,  
14 Paul Thomas, Ryan Tibble, Jason Town, Kaitlyn Tsai, Fatima Ugur, Douglas R. Wassermann,  
15 Alexander Wolff, Taia Wu

16 *Faculty/Staff:* Derrick Bogdanoff, Jennifer Li, Kurt S. Thorn, Shane O’Conchúir, Danielle L.  
17 Swaney, Eric D. Chow, Hiten Madhani, Sy Redding, Daniel N. Bolon, Tanja Kortemme, Joseph  
18 L. DeRisi, Martin Kampmann\*, James S. Fraser\*

19 \*corresponding authors: [martin.kampmann@ucsf.edu](mailto:martin.kampmann@ucsf.edu), [jfraser@fraserlab.com](mailto:jfraser@fraserlab.com)

20

21 **Abstract (150 words)**

22 Although the primary protein sequence of ubiquitin (Ub) is extremely stable over evolutionary  
23 time, it is highly tolerant to mutation during selection experiments performed in the laboratory.  
24 We have proposed that this discrepancy results from the difference between fitness under  
25 laboratory culture conditions and the selective pressures in changing environments over  
26 evolutionary time scales. Building on our previous work (Mavor et al 2016), we used deep  
27 mutational scanning to determine how twelve new chemicals (3-Amino-1,2,4-triazole, 5-  
28 fluorocytosine, Amphotericin B, CaCl<sub>2</sub>, Cerulenin, Cobalt Acetate, Menadione, Nickel Chloride,  
29 p-fluorophenylalanine, Rapamycin, Tamoxifen, and Tunicamycin) reveal novel mutational  
30 sensitivities of ubiquitin residues. We found sensitization of Lys63 in eight new conditions. In  
31 total, our experiments have uncovered a sensitizing condition for every position in Ub except  
32 Ser57 and Gln62. By determining the Ubiquitin fitness landscape under different chemical  
33 constraints, our work helps to resolve the inconsistencies between deep mutational scanning  
34 experiments and sequence conservation over evolutionary timescales.

35

36 **Builds on:** Mavor D, Barlow KA, Thompson S, Barad BA, Bonny AR, Cario CL, Gaskins G, Liu  
37 Z, Deming L, Axen SD, Caceres E, Chen W, Cuesta A, Gate R, Green EM, Hulce KR, Ji W,  
38 Kenner LR, Mensa B, Morinishi LS, Moss SM, Mravic M, Muir RK, Niekamp S, Nnadi CI,  
39 Palovcak E, Poss EM, Ross TD, Salcedo E, See S, Subramaniam M, Wong AW, Li J, Thorn KS,  
40 Conchúir SÓ, Roscoe BP, Chow ED, DeRisi JL, Kortemme T, Bolon DN, Fraser JS.  
41 Determination of Ubiquitin Fitness Landscapes Under Different Chemical Stresses in a  
42 Classroom Setting. *eLife*. 2016.

43

44 **Impact Statement:** We organized a project-based course that used deep mutational scanning  
45 in multiple chemical conditions to resolve the inconsistencies between tolerance to mutations in  
46 laboratory conditions and sequence conservation over evolutionary timescales.

47

## 48 **MAIN TEXT**

49

### 50 **Introduction**

51

52 Ubiquitin (Ub) is an essential eukaryotic protein acting as post-translational modification to  
53 mediate the degradation of ~80% of the proteome and regulate protein localization and activity.  
54 (Yau and Rape, 2016). The amino acid sequence of ubiquitin has been strikingly stable  
55 throughout evolutionary time: between yeast and human, there are only 3 amino acid changes  
56 (96% sequence identity) (Finley et al., 2012; Roscoe et al., 2013). However, deep mutational  
57 scanning experiments in yeast have revealed that Ub is surprisingly robust to sequence  
58 changes, with 19 positions freely mutating to almost any other amino acid without a loss of  
59 fitness (Roscoe et al., 2013).

60

61 To interrogate the dichotomy between the mutational robustness and the strong sequence  
62 conservation of Ub, we initially hypothesized that sensitivities to mutations at new positions  
63 could be revealed by growing yeast under different selective pressures in a classroom setting.  
64 To test this idea, we previously determined the fitness landscape of ubiquitin in four different  
65 chemical perturbations (DTT, caffeine, hydroxyurea (HU), and MG132) (Mavor et al., 2016). We  
66 showed that three of the perturbations (DTT, caffeine and HU) sensitize a shared set of  
67 positions to mutation. Under standard laboratory culture conditions, these fitness defects are  
68 buffered and undetectable. Conversely, we showed that the proteasome inhibitor MG132  
69 increases the mutational robustness of the ubiquitin sequence landscape. Inhibiting the  
70 proteasome reduces protein turnover through the same pathway as mutations in ubiquitin,  
71 leading to an alleviating interaction between MG132 and many of the mutant alleles. However,  
72 12 of the 19 residues of the tolerant face defined by (Roscoe et al., 2013) of Ub could still be  
73 freely mutated, suggesting that the environmental conditions constraining these positions were  
74 not sampled by these four perturbations.

75

76 To build on these results, we again involved the first-year graduate students in UCSF's iPQB  
77 and CCB programs to determine the fitness landscape of ubiquitin in distinct environments. We  
78 chose twelve new chemical perturbations (3-Amino-1,2,4-triazole (3-AT), 5-fluorocytosine (5-  
79 FC), Amphotericin B (AmpB), CaCl<sub>2</sub>, Cerulenin, Cobalt Acetate (Cobalt), Menadione, Nickel  
80 Chloride (Nickel), p-Fluorophenylalanine (p-FP), Rapamycin, Tamoxifen, and Tunicamycin),  
81 which impose a wide range of stresses upon the cell, including osmotic shock, protein folding  
82 stress, and DNA damage. Our results represent an important next step towards how deep  
83 mutational scanning can be used to explain the evolutionary constraints on sequence  
84 conservation patterns.

85

86

87

## 88 Results

89

90 *Distinct chemical treatments can sensitize or increase robustness of Ub to mutation*

91

92 We calculated distribution of fitness changes using the EMPIRC-BC method (Mavor et al. 2016)  
93 across each pairwise environmental comparison (**Figure 1**) and examined the response of  
94 individual residues (**Figure 2**). Treatment with 3-AT, AmpB, CaCl<sub>2</sub>, Cobalt, and p-FP shifted the  
95 residual distribution towards the reduced fitness (left shift in **Figure 1**) when compared to the  
96 distribution of two DMSO treatments. The sensitizing compounds (3-AT, AmpB, CaCl<sub>2</sub>, Cobalt,  
97 and p-FP) have a dominant effect at positions near hydrophobic patch residues (8, 44, 70) and  
98 the C-terminus (**Figure 2**), which is similar to that previously observed after treatment by  
99 Caffeine, DTT, or HU (Mavor et al. 2016).

100

101 In contrast, 5-FC, Cerulenin, Menadione, and Tamoxifen led to more residues having fitness  
102 greater than in DMSO (right shift in **Figure 1**). Treatment with Cerulenin or Menadione acted  
103 similarly to treatment with MG132; most positions in Ub have mildly increased robustness to  
104 mutation, with a few specific mutations appearing either sensitive or tolerant (**Figure 2**).  
105 However, 5-FC and Tamoxifen show strong mutational robustness at the biologically important  
106 positions (Mavor et al) adjacent to the hydrophobic patch and C-terminus (**Figure 2**).

107

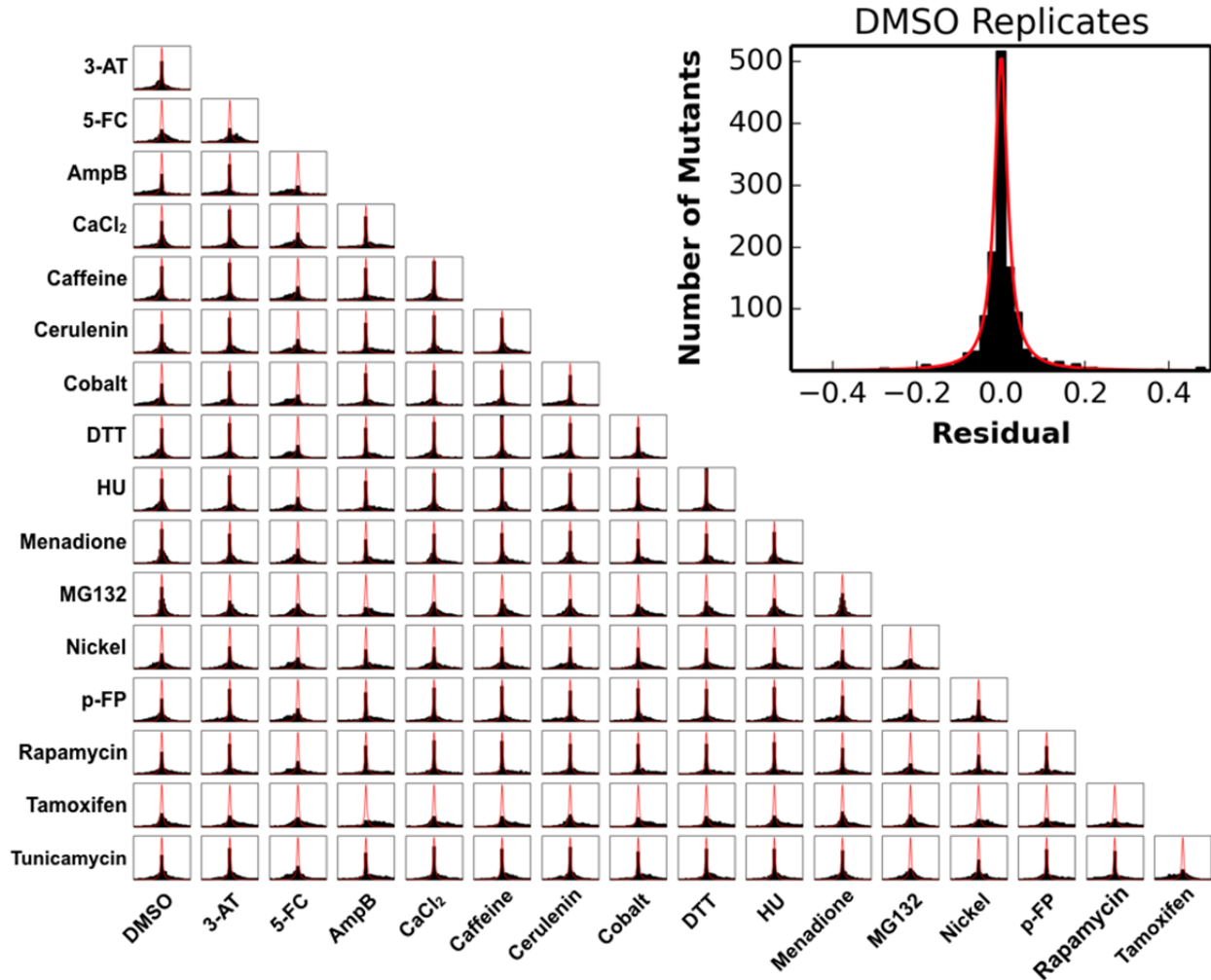
108 We observed distinct fitness landscapes for Nickel, Rapamycin, Tunicamycin. These treatments  
109 caused large tails in the distribution towards increased and decreased fitness, suggesting that  
110 these chemicals induce a unique pattern of sensitization and robustness for different mutants  
111 (**Figure 1**). For example, positions 40 and 58 become more tolerant to mutation when cells are  
112 exposed to Nickel, but positions 32 through 35 become strongly sensitized. Additionally, several  
113 positions show a diverse response to mutation to specific residue types when cells are treated  
114 with Nickel (**Figure 2**). For example, Gln2 has an increased relative fitness when mutated to  
115 Asn or a positive residue, but a decreased relative fitness when mutated to small hydrophobic or  
116 negative residues. Rapamycin and Tunicamycin have many residues where the mutational  
117 effects mirror each other (**Figure 2**). For positions 2, 32, 35, 37, and 38 Rapamycin treatment  
118 desensitizes the position to mutation while Tunicamycin treatment causes sensitization. At  
119 position 63 we observe the opposite, with Tunicamycin desensitizing and Rapamycin sensitizing  
120 the position.

121

122

123

124  
125



126  
127

128 **Figure 1:** The residuals between data sets reveal global patterns: Inset shows the Lorentzian fit to biological  
129 replicates of DMSO in red and data in black. When treatments are compared to DMSO (first column), 3-AT, AmpB,  
130 CaCl<sub>2</sub>, Cobalt, and p-FP shift the residual distribution to the left. This highlights the increased sensitivity to mutation.  
131 In contrast, 5-FC, Cerulenin, Menadione, and Tamoxifen shift the distribution to the right, highlighting the strong  
132 alleviating interactions caused by these treatment. For Nickel, Rapamycin, Tunicamycin we observe long tails on  
133 either side of the distribution, highlighting that these treatments induce both strong sensitizing and strong alleviating  
134 effects on mutations to Ub.

135  
136



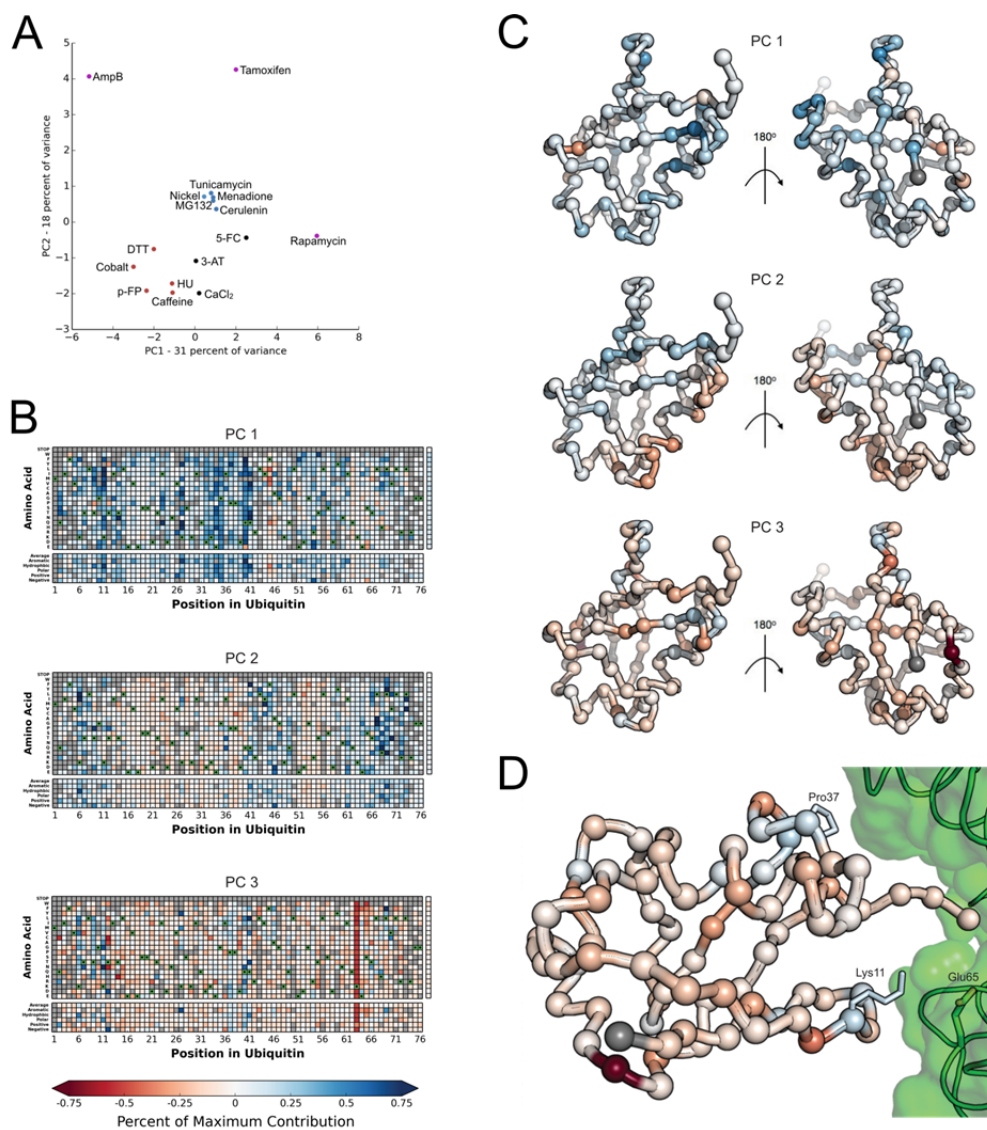
145 *Principal Component Analysis of Deep Mutational Scanning Data Across Chemical*  
146 *Perturbations*

147  
148 To reveal whether common responses were driving the differences between treatments, we  
149 performed principal component analysis on the difference fitness data (**Figure 3**). We focused  
150 on the first three principal components, which collectively explain 60 percent of the variance.  
151 Projecting the treatments onto the first two principal components shows that the sensitizing  
152 (Caffeine, Cobalt, DTT, HU, p-FP) and desensitizing treatments (Cerulein, Menadione,  
153 MG132, Nickel, Tunicamycin) form independent clusters. Treatment with AmpB, Rapamycin, or  
154 Tamoxifen appear as outliers in this space.

155  
156 To examine the mechanistic basis for these clusters, we mapped the contribution of each  
157 mutation to each of the first three principal components (PCs). PC1 appears as mild positive  
158 contributions for most mutations, with the strongest positive signals appearing at residues 11,  
159 27, 40 and 41. Interestingly, the strongest negative contributions appear at Phe45, a large core  
160 residue. PC2 separates the previously described tolerant face of Ub from the sensitive face,  
161 which includes the “hydrophobic patch”. Positions close to the hydrophobic patch residues have  
162 a positive contribution to PC2, while positions on the opposite face have negative contributions.

163  
164 PC3 is dominated by the response to mutation at Lys63, a key poly-Ub linkage site. Lys63  
165 linked poly-Ub is an important regulator of the DNA damage response in yeast and is also  
166 involved in efficient endocytosis and cargo sorting to the vacuole in yeast (Erpapazoglou et al.,  
167 2014). To investigate PC3, we used Rosetta to calculate the ddG of interaction for various  
168 complexes involved in Lys63 linked poly-Ub, including the closed and open forms of Lys63  
169 linked di-Ub and the donor and acceptor ubiquitin poses on the MMS/Ubc13 heterodimer, the  
170 E2 that catalyzes Lys63 linked poly-Ub in yeast. We binned the calculated ddG values in  
171 stabilizing ( $ddG < -0.75$ ) and destabilizing ( $ddG \geq 0.75$ ). We then calculated the contributions  
172 of each mutation to PC3 and compared the two distributions. Positions that destabilize this  
173 interface (mutations at Lys11 and Pro37) are enriched in positive contributions to the PC. This  
174 argues that conditions that require building K63-linked poly-Ub chains (those where position 63  
175 is sensitized) have an increased relative fitness at mutations that destabilize the donor ubiquitin  
176 pose. Interestingly, when Lys11 is mutated to Arg, there is a strong negative contribution to  
177 PC3. This is the only mutation at position 11 that is predicted to stabilize the interface, likely due  
178 to Lys11 participating in a salt-bridge with Glu65 of Ubc13.

179  
180  
181

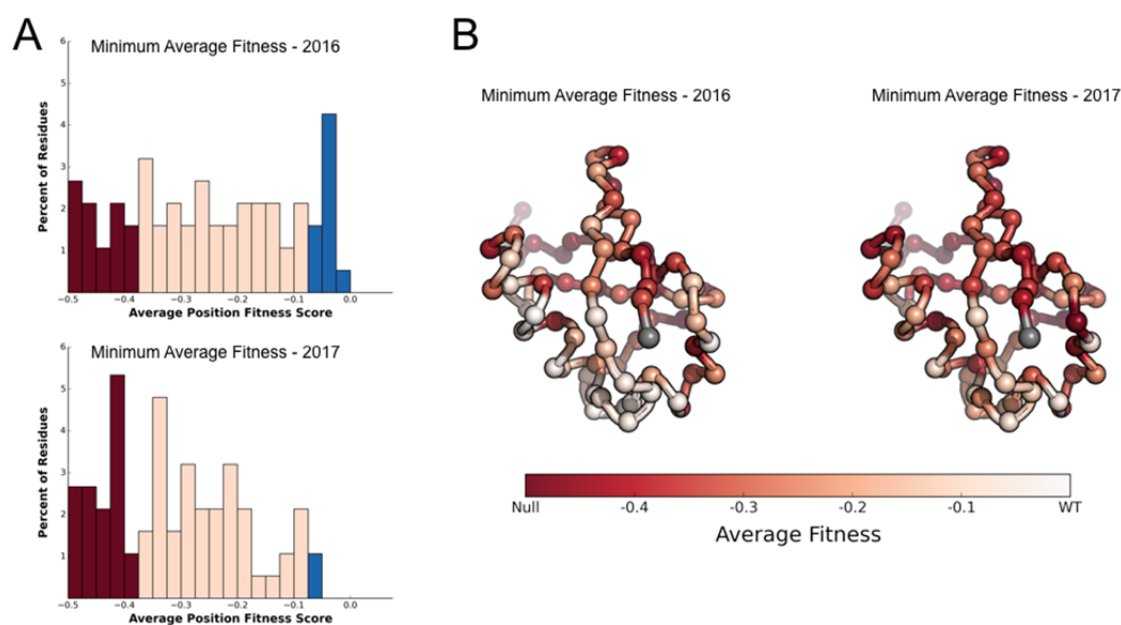


182  
183  
184  
185  
186  
187  
188  
189  
190  
191  
192  
193  
194  
195  
196  
197  
198  
199  
200

**Figure 3:** Principal component analysis reveals specific signals related to K63 incorporation: (A) The first two principal components reveal a sensitizing cluster plotted in red and an alleviating cluster shown in blue. Three strong outliers are shown in Purple. Treatment with 3-AT, 5-FC or CaCl<sub>2</sub> appear between clusters with positive values for PC1 and negative values for PC2. (B) The contribution of each mutation to each principal component was visualized as a heat map. The percentage of the maximum contribution to that principal component is represented from 75% (Blue) to -75% (Red). (i) PC1 is related to the general sensitivity of Ub mutants to the perturbation. Negative values in the PC correspond to greater sensitization. Strikingly, this general sensitization is coupled to robustness to some mutations at the core residue Phe45. (ii) PC2 differentiates “Sensitive Face” residues (positive contributions) from “Tolerant Face” residues (Negative Contributions). (iii) PC3 reveals mutations that are correlated with sensitization of Lys63. (C) The average contribution of each mutation at each position was plotted from 75% (Blue) to -75% (Red) on the Ub monomer structure for PC1 (A), PC2 (B), and PC3 (C). (D) Rosetta  $\Delta\Delta G$  calculations revealed that mutations that strongly destabilize the donor Ub pose on the MMS/Ubc13 (2GMI) heterodimer are localized to Lys11 and Pro37 (shown in sticks). In the case of Lys11, all mutations other than that to Arg destabilize the interface suggesting a salt-bridge between Lys11 and Glu65 of Ubc13 (shown in green sticks) Ubiquitin residues are colored by the contribution to PC3 as in panel C iii.



201  
202  
203 *Deep mutational scanning in different chemical environments reveals constraints on most*  
204 *residues*  
205  
206 To continue our efforts in explaining the evolutionary constraints that lead to the exquisite  
207 conservation of Ub, we selected the condition with the minimum of average fitness at each  
208 position as the “minimum average fitness”. We then binned the minimum average fitness for each  
209 position into sensitive ( $\leq -0.35$ ), intermediate ( $-0.35$  to  $-0.075$ ) and tolerant ( $\geq -0.075$ ) (**Figure 4**).  
210 Previously we showed sensitization at all but twelve positions in Ub (Mavor et al., 2016). By  
211 expanding the number of perturbations, we now show all but two positions, Ser57 and Gln62,  
212 are sensitized in at least one condition.



213  
214 **Figure 4:** New perturbations reveal constraints on all but two Ub positions: (A) Positions were  
215 binned into tolerant ( $\geq -0.075$  - Blue), intermediate ( $< -0.075$  to  $> -0.35$  - Pink) and sensitive ( $\leq -0.35$  - Red) and the  
216 distributions plotted for each perturbation. Calculating the minimum average fitness reveals how the new  
217 perturbations reveal additional constraints on the Ub fitness landscape. (B) Average position fitness scores mapped  
218 onto ubiquitin. (i) Minimum average fitness score in DMSO, Caffeine, DTT, HU, and MG132 (ii) Minimum average  
219 fitness score in all conditions. C-alpha atoms are shown in spheres and the residues are colored according to  
220 average fitness. Met1 is colored grey.

## 221 222 Discussion

223  
224 No single perturbation can replicate the diverse pressures that natively constrain protein  
225 evolution. We can now rationalize many of the constraints that have led to the extreme  
226 sequence conservation of Ub by examining the fitness landscape under a large variety of  
227 conditions, including redox stress, osmotic stress, protein folding stress, DNA damage, ER  
228 stress, and anti-fungals. Notable exceptions are residues Ser57 and Gln62, which are not  
229 sensitive to mutation under any condition yet tested.

230

231 Of the newly revealed sensitivities, perhaps the most exciting is the sensitization of Lys63,  
232 captured by PC3, in eight conditions. Lys63-linked poly-Ub participates in the response to DNA  
233 damage, where Lys63-linked poly-Ub is catalyzed on PCNA to induce error-free postreplication  
234 repair (Zhang et al., 2011), and in endocytosis, where efficient endocytosis in cargo sorting to  
235 the vacuole requires Lys63-linked poly-Ub chains (Erpapazoglou et al., 2014).

236

237 In contrast, we previously observed an increase in mutational robustness at Lys63 in DTT  
238 treatment, a reducing agent that interferes with ER protein folding. Interestingly, we also  
239 observe increased robustness under Tunicamycin treatment, a compound that interferes with  
240 ER protein folding via a distinct mechanism (Chawla et al., 2011). This result suggests an  
241 epistatic interaction between Lys63 signalling and the unfolded protein response, which may  
242 complement the suggested role of Lys11 under high (30mM) DTT treatment (Xu et al., 2009).  
243 The Lys11Arg mutant is specifically sensitized in Tunicamycin suggesting that the origin of this  
244 effect may be structural, rather than due to a requirement for Lys11-linked poly-Ub.

245

246 In addition to the increased robustness at Lys63, Tunicamycin treatment leads to a unique  
247 increase in mutational robustness at several other positions, including Lys6, Lys11, and Lys33.  
248 These results address a major challenge in Ub biology: understanding the biological role of  
249 distinct poly-Ub species. While the mutational tolerance pattern at Lys6 and Lys11 appear to be  
250 due to disrupting a salt-bridge, the increased robustness at Lys33 suggests a connection  
251 between Tunicamycin and Lys33 linked poly-Ub. We observed, further, but less conclusive,  
252 Lysine-specific effects for Lys27, Lys29, and Lys33 under treatment with AmpB, Cobalt, or  
253 Nickel.

254

255 Finally, these experiments continue to highlight the success of project-based courses. Over the  
256 course of 6-8 weeks, first year graduate students in UCSF's CCB and iPQB programs  
257 generated and analyzed these data using their own computational pipelines. We believe that the  
258 Ub yeast library is an ideal system for such project-based courses due to the wide range of  
259 stress responses mediated by the system and the vastness of chemical space. It is our hope  
260 that other graduate programs can offer similar project based classes in the future and our  
261 regents are available to further that goal.

262

263

264

265  
266  
267  
268  
269  
270  
271  
272  
273  
274  
275  
276  
277  
278  
279  
280  
281  
282  
283  
284  
285  
286  
287  
288  
289  
290  
291  
292  
293  
294  
295  
296  
297  
298  
299  
300  
301  
302  
303  
304

## Methods

*Additional material is available:*

PUBS website ([www.fraserlab.com/pubs](http://www.fraserlab.com/pubs))

GitHub (<https://github.com/fraser-lab/PUBS>).

Raw Sequencing reads are made available via SRA (SRA Accession Number:SRP070953)

*Updated Methods from Mavor et al 2016:*

For each compound, we determined the the chemical concentrations that inhibited SUB328 (WT Ub) growth by 25% (3-Amino-1,2,4-triazole - 50 mM, 5-fluorocytosine - 1.25 ug/mL, Amphotericin B - 400 nM, CaCl<sub>2</sub>- 500mM, Cerulenin - 4.5 uM, Cobalt Acetate - 600 uM, Menadione- 500 uM, Nickel Chloride - 400 uM, p-Fluorophenylalanine - 800 ug/mL, Rapamycin - 200 nM, Tamoxifen - 25 uM, and Tunicamycin- 1 mg/mL). Other growth, sequencing, and data processing methods are unchanged.

*Principal Component Analysis:*

PCA was performed using scikit-learn (version 0.18.1) in Python with the following parameters:

```
PCA(copy=True, iterated_power='auto', n_components=None, random_state=None,
    svd_solver='auto', tol=0.0, whiten=False)
```

For each compound, the difference in fitness between DMSO and perturbation was calculated. PCA was performed on these 16 vectors. In the case of a missing observation for any mutant and positions, that mutant and position was excluded from the analysis.

*ROSETTA ddG predictions:*

Interface ddG predictions were generated using the Rosetta macromolecular modeling suite, which is freely available for academic use. The git version used was 12e38402d9. For each amino acid position in the MMS/Ubc13 heterodimer, the interface ddG protocol was run as follows: 1) Minimize (with constraints to the starting coordinates) the starting wildtype structure (PDB ID: 2GMI). 2) Generate an ensemble of 50 conformational states using Rosetta's backrub application (10,000 trials, temperature 1.2), using residues in an 8Å radius of the specified amino acid position as backrub pivot residues. 3) Repack, or repack and mutate the side chains of the specified amino acid and the pivot residues from step 2. 4) Minimize (with constraints) the wild type and mutant structures generated in step 3. 5) For each structure *i* (of 50), we calculate the ddG score as follows:

$$\Delta\Delta G_{bind} = (\Delta G_{MUT\ complex\ i} - \Delta G_{MUT\ psrtner\ Ai} - \Delta G_{MUT\ partner\ Bi}) - (\Delta G_{WT\ complex\ i} - \Delta G_{WT\ partner\ Ai} - \Delta G_{WT\ partner\ Bi})$$

We then average all 50  $\Delta\Delta G_{bind}$  scores to obtain the final predicted value.

305  
306  
307  
308  
309  
310  
311  
312  
313  
314  
315  
316  
317  
318  
319  
320  
321  
322  
323  
324  
325  
326  
327

## **Acknowledgements**

We acknowledge: administrative support from Rebecca Brown, Julia Molla, and Nicole Flowers; technical support from Jennifer Mann and Manny De Vera; gifts from David Botstein, and Illumina; and helpful discussions with Nevan Krogan and Ron Vale. The Project Lab component of this work is specifically supported by an NIBIB T32 Training Grant, 'Integrative Program in Complex Biological Systems' (T32-EB009383). UCSF iPQB and CCB Graduate programs are supported by US National Institutes of Health (NIH) grants EB009383, GM067547, GM064337, and GM008284, HHMI/NIBIB (56005676), UCSF School of Medicine, UCSF School of Pharmacy, UCSF Graduate Division, UCSF Chancellor's Office, and Discovery Funds. WC, EMG, LRK, LSM, PS, TLN, NJR and FSU are supported by NSF Graduate Research Fellowships. DNB is supported by NIH GM112844. TK is supported by NIH R01 GM117189, R01 GM110089 and NSF MCB-1615990. HDM is supported by NIH R01 GM071801, R01 AI100272 , R01 AI120464, R56 AI126726 and the Chan Zuckerberg Biohub. MK is supported by an NIH Director's New Innovator Award (NIH/NIGMS DP2 GM119139), an Allen Distinguished Investigator Award (Paul G. Allen Family Foundation), a Stand Up to Cancer Innovative Research Grant, NIH K99/R00 CA181494, the Tau Center Without Walls (NIH/NINDS U54 NS100717), the Chan Zuckerberg Biohub and the Paul F. Glenn Center for Aging Research. JSF is a Searle Scholar, Pew Scholar, and Packard Fellow, and is supported by NIH OD009180.

328

329 **REFERENCES**

- 330 Chawla, A., Chakrabarti, S., Ghosh, G., and Niwa, M. (2011). Attenuation of yeast UPR is  
331 essential for survival and is mediated by IRE1 kinase. *J. Cell Biol.* *193*, 41–50, PMID:  
332 PMC3082189.
- 333 Erpapazoglou, Z., Walker, O., and Haguenuer-Tsapis, R. (2014). Versatile roles of k63-linked  
334 ubiquitin chains in trafficking. *Cells* *3*, 1027–1088, PMID: PMC4276913.
- 335 Finley, D., Ulrich, H.D., Sommer, T., and Kaiser, P. (2012). The ubiquitin-proteasome system of  
336 *Saccharomyces cerevisiae*. *Genetics* *192*, 319–360, PMID: PMC3454868.
- 337 Mavor, D., Barlow, K., Thompson, S., Barad, B.A., Bonny, A.R., Cario, C.L., Gaskins, G., Liu, Z.,  
338 Deming, L., Axen, S.D., et al. (2016). Determination of ubiquitin fitness landscapes under  
339 different chemical stresses in a classroom setting. *Elife* *5*, PMID: PMC4862753.
- 340 Roscoe, B.P., Thayer, K.M., Zeldovich, K.B., Fushman, D., and Bolon, D.N.A. (2013). Analyses  
341 of the effects of all ubiquitin point mutants on yeast growth rate. *J. Mol. Biol.* *425*, 1363–1377,  
342 PMID: PMC3615125.
- 343 Xu, P., Duong, D.M., Seyfried, N.T., Cheng, D., Xie, Y., Robert, J., Rush, J., Hochstrasser, M.,  
344 Finley, D., and Peng, J. (2009). Quantitative proteomics reveals the function of unconventional  
345 ubiquitin chains in proteasomal degradation. *Cell* *137*, 133–145, PMID: PMC2668214.
- 346 Yau, R., and Rape, M. (2016). The increasing complexity of the ubiquitin code. *Nat. Cell Biol.*  
347 *18*, 579–586.
- 348 Zhang, W., Qin, Z., Zhang, X., and Xiao, W. (2011). Roles of sequential ubiquitination of PCNA  
349 in DNA-damage tolerance. *FEBS Lett.* *585*, 2786–2794.

350

351

352

353

354